Genetic and Epigenetic Modeling of the Origins of Multidrug-Resistant Cells in a Human Sarcoma Cell Line

Kevin G. Chen,[1,2] Yan C. Wang,[1] Marci E. Schaner,[1,2] Brian Francisco,[1] George E. Durán,[1] Dejan Juric,[1] Lyn M. Huff,[3] Hesed Padilla-Nash,[4] Thomas Ried,[4] Tito Fojo,[3] and Branimir I. Sikic[1,2]

[1]Division of Oncology, Department of Medicine and [2]Program in Cancer Biology, Stanford University School of Medicine, Stanford, California; [3]Medicine Branch, and [4]Genetics Branch of the National Cancer Institute, NIH, Bethesda, Maryland

Abstract

The origin of drug-resistant cells in human cancers has been a fundamental problem of cancer pharmacology. Two major contrasting hypotheses (genetics versus epigenetics) have been proposed to elucidate the mechanisms of acquired drug resistance. In this study, we answer these fundamental questions through investigation of the genetic and epigenetic pathways that control the origin of *ABCB1* (*MDR1*) gene activation with acquired multidrug resistance in drug-sensitive human sarcoma (MES-SA cells). The genetic and epigenetic bases of this selected activation involve the initiation of transcription at a site 112 kb upstream of the *ABCB1* proximal promoter (P1) in the drug-resistant cells. This activation was associated with a chromatin-remodeling process characterized by an increase in acetylated histone H3 within a 968-bp region 5′ of the *ABCB1* upstream promoter. These alterations provide both genetic and epigenetic susceptibility for *ABCB1* expression in drug-resistant cells. Complete activation of the *ABCB1* gene through the coding region was proposed by interactions of selected *trans*-alterations or epigenetic changes on the *ABCB1* proximal promoter, which occurred during initial drug exposure. Thus, our data provide evidence for a major genomic alteration that changes the chromatin structure of the *ABCB1* upstream promoter via acetylation of histone H3 initiating *ABCB1* activation, further elucidating the genetic and epigenetic bases that determine chemotherapeutic response in drug-resistant derivatives of MES-SA cells. (Cancer Res 2005; 65(20): 9388-97)

Introduction

Scientists have attempted to determine the origin of drug-resistant cells for decades. Two hypotheses have been proposed to account for drug resistance mechanisms in cancer cells. One hypothesis is the occurrence of random mutational events by which a drug-resistant variant arises spontaneously from sensitive cells. Another hypothesis is epigenetic changes (e.g., induction of gene expression via methylation or acetylation) resulting in resistance to cytotoxic insults. Whether drug-resistant cells originate from spontaneous mutations or by induction has been a controversial topic, with, to date, no definitive resolution (1–5).

Fluctuation analysis provides a powerful genetic tool to differentiate a spontaneous mutational event from an epigenetic alteration (1–4). The major drawback of this analysis is that conclusions are mainly based on ANOVA and mean of surviving clones. No direct molecular evidence can be obtained. Moreover, application of fluctuation analysis to human cancer cells is a major challenge due to the genetic complexity and heterogeneity of cancer cells compared with that of bacteria, all of which make the interpretation of data more difficult.

To circumvent the above obstacles and model the genetic steps of generating multidrug-resistant (MDR) cells, we have established a highly reliable and reproducible system from the human sarcoma cell line MES-SA to perform fluctuation and molecular analyses (6–9). Moreover, the MDR phenotype mediated by the ATP-binding cassette transporter ABCB1/P-glycoprotein is also a well-characterized drug-resistant mechanism (reviewed in refs. 10, 11). Significant progress has been made to delineate the mechanisms underlying *ABCB1* expression in normal and tumor cells, particularly in MDR cellular models (reviewed in ref. 12). The unique set of *ABCB1* mutants derived from MES-SA cells represent a valuable model system to dissect the genetic and molecular elements that control the origins of multidrug resistance in cancer cells.

In this study, we provide direct genetic and epigenetic evidence for the origin of acquired multidrug resistance from drug-sensitive cancer cells. We have established a molecular/genetic model to dissect genetic and epigenetic steps that are required for *ABCB1* activation under stringent drug selection. In this model, we propose that a major genomic alteration provides genetic bases for the initiation of *ABCB1* activation (generating a partially activated *ABCB1* status) via an epigenetic modification of chromatin structure. Interplay between spontaneous mutations and selected epigenetic alterations contributes to complete activation of the *ABCB1* gene.

Materials and Methods

Cellular models. Cell Culture, development, and characterization of the sublines of a human uterine sarcoma (MES-SA) were previously described (Table 1; refs. 6, 9, 13). Cells used in this work include a panel of drug-resistant subclones derived by single exposures of MES-SA cells to either doxorubicin or vinblastine or etoposide (VP-16).

Single-step selection of the MES-SA subline (MFS). Single-step selection of the subclonal MES-SA cells (MFS) with vinblastine has been previously described (9). At that time, MFS cells were also seeded into twelve 96-well plates (1.7×10^6 cells per plate) and six plates treated with either 80 nmol/L doxorubicin or 0.5 μmol/L VP-16 for 2 weeks. These selection conditions were chosen based on the IC_{50} of MES-SA cells and the need to minimize the proportion of cells surviving based on stochastic or epigenetic mechanisms. Surviving colonies were allowed to grow for another 2 to 3 weeks and counted. Wells containing single colonies were harvested and expanded in drug-free medium for further studies.

Note: Supplementary data for this article are available at Cancer Research Online (http://cancerres.aacrjournals.org/).

Requests for reprints: Kevin G. Chen, NIH Stem Cell Unit, National Institute of Neurological Disorders and Stroke, NIH, Room 1000, Building 37, Convent Drive, Bethesda, MD 20892. Phone: 301-402-8118; Fax: 301-480-1022; E-mail: cheng@mail.nih.gov.

doi:10.1158/0008-5472.CAN-04-4133

Table 1. Drug sensitivity phenotype of MES-SA drug-resistant variants (fold resistance)

Clones	Vinblastine	Doxorubicin	VP-16
Controls			
MES-SA	1	1	1
MES-SA/FS (MFS)*	1	1	1
Drug Selected Variants			
MES-SA/2B-E3 †	21	5	3
MES-SA/3B-B9 †	5	6	3
MES-SA/10B-E2 †	8	6	3
MFS/VL20-4.1 ‡	70	38	5
MFS/DS-5§	45	5	10
MES-SA/DOX6D‖	4	2	2
MES-SA/VP6D¶	1	1	2
MES-SA/VP12D¶	2	2	4
Dx5**	243	80	42

NOTE: Fold resistance was determined by the 3-(4,5-dimethylthiazol-2-yl)-2,5-diphenyltetrazolium bromide cytotoxicity assay (6).
Abbreviations: 6D, drug exposure for 6 d; 12D, drug exposure for 12 d.
*A subclone of MES-SA cells was isolated by limiting dilution method (9, 14).
† DSMs of MES-SA cells were isolated via fluctuation analysis (6). Three representative clones of 13 populations are shown.
‡ VSMs were derived from the MES-SA subclone cells (MFS; ref. 9). A representative clone of a population of eight is shown.
§MFS/DSM (80 nmol/L) cells were generated in this study. One representative clone of each selection is shown.
‖MES-SA cells were undergone with sublethal induction/selection by doxorubicin (40 nmol/L).
¶MES-SA cells were undergone with sublethal induction/selection by VP-16 (0.5 μmol/L).
**Multistep doxorubicin-selected MDR cells from MES-SA cells (13).

Induction or sublethal induction of *ABCB1* expression in MES-SA cells. To determine whether *ABCB1*/P-glycoprotein could be induced in these sarcoma cells, bulk populations of MES-SA cells were either treated by 80 nmol/L doxorubicn for 24, 48, and 72 hours or treated for 24 hours in escalated doxorubicin concentrations (0.04, 0.08, 0.25, 1, 2, and 4 μmol/L). For sublethal induction, MES-SA cells were seed into two 80-cm^2 flasks, and each was treated with either 80 nmol/L doxorubicin or 0.5 μmol/L VP-16 for 6 days. Then the cells were maintained in drug-free medium for 2 weeks. The surviving cells were harvested and characterized for *ABCB1*/P-glycoprotein expression, drug sensitivity, and other phenotypic changes as previously described (6, 9).

Cellular drug sensitivity assays. The cellular drug sensitivity was evaluated by the 3-(4,5-dimethylthiazol-2-yl)-2,5-diphenyltetrazolium bromide assay in triplicate or quadruplicate as described (6).

Flow cytometry. P-glycoprotein expression and function were assessed by two-color flow cytometry using double staining of cells with both the monoclonal antibody UIC2 and rhodamine-123 (Rh-123) as described (6, 13).

Southern blotting. Extraction of genomic DNAs and Southern blotting analysis were done according to a previously described method (14).

RNase protection assay. Total RNAs from control cells and MDR variants were hybridized with an antisense RNA probe generated by SP6 RNA polymerase from a 982-bp *Pst*I-*Pst*I genomic fragment of the *ABCB1* promoter. The RNase protection assay was done by hybridizing total RNA with 2×10^5 cpm of the antisense RNA probe as described (15).

Rapid amplification of 5′ cDNA ends. The rapid amplification of 5′ cDNA ends (5′-RACE) kit (Life Technologies/Bethesda Research Laboratories, Gaithersburg, MD) was used with mRNA isolated from 10B-E2 cells using the FastTrack 2.0 mRNA Isolation Kit (Invitrogen, Carlsbad, CA). Reverse transcription from the isolated mRNAs was then carried out using a gene-specific primer in exon 1 (GSP-1, Table 2). PCR was carried out under the following conditions: 94°C for 4 minutes, 94°C for 1 minute, 55°C for 1.5 minutes, 72°C for 2 minutes (35 cycles); 72°C extension for 10 minutes using a gene-specific primer (GSP-2, Table 2) and the anchor primer from Life Technologies/Bethesda Research Laboratories. Following the initial PCR reaction, a nested PCR was carried out using the reverse primer GSP-3 (Table 2), an *ABCB1*-specific primer, and an abridged universal anchor primer provided with the kit. The products from nested PCR were subcloned into the pGEM-T vector (Promega Corp., Madison, WI) and sequenced at the Stanford University Sequencing Facility (Stanford, CA).

Conventional PCR. Both total RNAs and genomic DNAs were used for RCR analyses. Total RNA isolation and reverse transcriptase-PCR (RT-PCR) were done essentially as previously reported (6, 13). The different batches of RNA samples were assayed by PCR without reverse transcription to rule out genomic DNA contamination (data not shown). The primers for upstream mRNA detection were designed according to both the sequences derived from the 5′-RACE experiments and the published sequences (accession no. AC002457). The EC-94 forward primer is located at the beginning of exon −1 (94 bp) of the *ABCB1* gene (Table 2). The *ABCB1* +82 reverse primer is located at +82 relative to the transcription start site (+1) of the *ABCB1* promoter (Table 2). PCR was carried out as previously described (6, 13). The expected size of the PCR product is 370 bp, designated as ut370.

Real-time PCR. Quantitative real-time PCR using SYBR Green dye was done to detect mRNA expression and to verify the presence or absence of genomic sequence in chromatin immunoprecipitation assays in MES-SA and its drug-selected cell lines. The primers were designed according to the published sequences of the BAC clone CTB-60P12 (accession no. AC002457), synthesized in the Stanford University Pan Facility, and summarized in Table 2. Glyceraldehyde-3-phosphate dehydrogenase was used as an internal control for the above assays. The final 20-μL reaction mixture included 300 nmol/L of each primer and 1× SYBR Universal PCR master mix (Applied Biosystems, Foster City, CA). Thermal cycling was done with 10 minutes at 95°C followed by 40 cycles of PCR amplification: 95°C for 15 seconds and 62°C for 1 minute in the ABI Prism 7900 detection systems (Applied Biosystems). Amplification efficiencies were determined by serial dilutions. All reactions were done in triplicate. Dissociation curves were recorded after each run to confirm the primer specificity.

Chromatin immunoprecipitation. Chromatin immunoprecipitation analysis of the chromatin status of both *ABCB1* far upstream and downstream regions was done using the Acetyl-Histone H3 Immunoprecipitation Assay Kit (Upstate Cell Signaling Solutions, Lake Placid, NY) according to the manufacturer's instructions. The detailed experimental procedures using the anti-acetyl-histone H3 antibody, a rabbit polyclonal IgG specific for acetyl-histone H3, are available at the web site of this company (http://www.upstate.com). Briefly, 2×10^6 cells were used for each reaction in this assay. Histones were cross-linked to DNA and sonicated to 200 to 1,000 bp. The size of sonicated DNA was examined by gel electrophoresis after reversion of cross-links. Cell samples were precleared with 80 μL of salmon sperm DNA/protein A agarose/50% slurry for 30 minutes at 4°C before the addition of 10 μg of α-acetyl-histone H3 or normal rabbit IgGs (negative control, Sigma-Aldrich Chemical Co., St. Louis, MO). The protein A/antibody/histone/DNA complex was formed via overnight incubation at 4°C with rotation. Histone-DNA cross-links were reversed by adding 20 μL of 5 mol/L NaCl to 500 μL of the sample and incubated at 65°C for 4 hours. DNAs were recovered by phenol/chloroform extraction and ethanol precipitation and then dissolved in 250 μL of water. Nine microliters of purified DNAs were used for real-time PCR as described above. PCR primers used to amplify both the upstream *ABCB1* and the *ABCB1* P1 promoter regions were listed in Table 2.

Transient transfection experiments and chloramphenicol acetyltransferase assays. The plasmids used for transient transfection experiments were prepared according to the QIAGEN protocol (Qiagen,

Valencia, CA) and electroporated into MES-SA and its drug-selected cells using Gene Pulser II (Bio-Rad Laboratories, Hercules, CA) as described (16). Chloramphenicol acetyltransferase (CAT) assays were done as described (16). CAT activity for each sample was normalized to β-galactosidase activity to account for differences in electroporation.

Results

The multidrug-resistant phenotype in doxorubicin single-step-selected mutants. We previously established doxorubicin single-step-selected mutants (DSMs) via fluctuation analysis, with

Table 2. Oligonucleotides used in PCR

Amplimers	Sequences/location	(+/− strand) Exp./figure no.
Primer pairs for the genes upstream of *ABCB1**		
RPIB9-F	^{1379}AGATCCAGGCCAGTCACAAG$^{1398(BC022520)}$	(+) RT-PCR/F.4B3
RPIB9-R	^{1478}TCCACAGAGGCCAAGTAATG$^{1459(BC022520)}$	(−) RT-PCR/F.4B3
MCFP-F	^{395}TTCAACAAATGCTTGCCTCA$^{414(AF125531)}$	(+) RT-PCR/F.4B2
MCFP-R	^{492}GTTGTTTTGGGCTTGGAGTC$^{473(AF125531)}$	(−) RT-PCR/F.4B2
Primers for *ABCB1* upstream sequences †		
ECW-2F	^{150548}AGGGAGGTTTCACATCACCA^{150529}	(−) ChIP/F.5D4
ECW-2R	^{150444}CCCATGCATCCGTTTATAGG^{150463}	(+) ChIP/F.5D4
ECW-3F	^{150024}ACCCCTGCCCTCACTAAACT^{150005}	(−) ChIP/F.5D4
ECW-3R	^{149940}GGGGGTCACTACCTTCTGGT^{149959}	(+) ChIP/F.5D4
ECW-1F	^{149940}CCTGGACCCAGCTTTCACTA^{149921}	(−) ChIP/F.5D4
ECW-1R	^{149857}AACGGGGCTCTCTCTTTGTT^{149876}	(+) ChIP/F.5D4
ECW-4F	^{149889}CGATCCGCCTAAGAACAAAG^{149870}	(−) ChIP/F.5A
ECW-4R	^{149799}AGAATGCATTTTGGAATCTGTG^{149820}	(+) ChIP/F.5A
ECW-5F	^{149720}TCATTTTTCTCTCTGTGACAGCTC^{149700}	(−) ChIP/F.5A
ECW-5R	^{149644}TTTTAGCACAAATTGAAGGAAGG^{149666}	(+) ChIP/F.5A
ECP/ECW-F	^{149376}TCATTTGAAGGTCTTCCCAGT^{149356}	(−) ChIP/F.5A
ECP/ECW-R	^{149227}TGGCTTAGGGATTGGGGTAT^{149246}	(+) ChIP/F.5A
ECP-2F	^{149236}CCCTAAGCCATGTAACTCTTCG^{149215}	(−) ChIP/F.5D3
ECP-2R	^{149120}TGACTATGGCTCCAAAGCAT^{149139}	(+) ChIP/F.5D3
ECP-3F	^{149172}CACCTTAGCAAAAAGATCACACA^{149150}	(−) ChIP/F.5A
ECP-3R	^{149078}GGAGGAAGGGTGGGAGTAGA^{149097}	(+) ChIP/F.5A
ECP-4F	^{149037}AAGCCTGCCTGCCTTAGTTC^{149018}	(−) ChIP/F.5A
ECP-4R	^{148941}TTCACAGGTAAAGAGTAATGATAGCC^{148966}	(+) ChIP/F.5A
Primers for the *ABCB1* upstream transcript ut370 †		
EC-94F	ATCGATCGGTCGACC^{148921}CTACTCTATTCAGATATTCTCCAGATTCC^{148893}	(−) RT-PCR/F.2E,3
ABCB1+82R	ATCGATCGGGATCC^{36470}TACTCCGACTTTAGTGGAAAGACCTAAAGG^{36499}	(+) RT-PCR/F.2E,3
Primers at the *ABCB1* P1 promoter region †		
GSP3	^{36676}CTGATTCCTCGAGAAACTGCGA^{36697}	(+) 5′ RACE/F.2D
GSP2	^{36632}AGCCTCACCACAGATGACT^{36650}	(+) 5′ RACE/F.2D
GSP1	^{36559}GGCTTCCTGTGGCAAAGAG^{36577}	(+) 5′ RACE/F.2D
P1-1F	^{36655}GGAGCAGTCATCTGTGGTGA^{36636}	(−) ChIP/F.5D5
P1-1R	^{36533}GAAGAGCCGCTACTCGAATG^{36552}	(+) ChIP/F.5D5
P1-2F	^{36655}GGAGCAGTCATCTGTGGTGA^{36636}	(−) ChIP/F.5D5
P1-2R	^{36561}CTTCCTGTGGCAAAGAGAGC^{36580}	(+) ChIP/F.5D5
P1-3F	^{36704}ACCTGTTTCGCAGTTTCTCG^{36685}	(−) ChIP/F.5D5
P1-3R	^{36630}TCAGCCTCACCACAGATGAC^{36649}	(+) ChIP/F.5D5
P1-4F	^{36719}CCTCCTGGAAATTCAACCTG^{36700}	(−) ChIP/F.5D5
P1-4R	^{36630}TCAGCCTCACCACAGATGAC^{36649}	(+) ChIP/F.5D5
P1-5F	^{36553}TCATTCGAGTAGCGGCTCTT^{36534}	(−) ChIP/F.5D5
P1-5R	^{36444}CCAAGACGTGAAATTTTGGAA^{36464}	(+) ChIP/F.5D5
ABCB1-F ‡	^{4204}GCTGGCACAGAAAGGCATCTA$^{4224(M14758)}$	(+) RT-PCR/F.4B1
ABCB1-R ‡	^{4273}CAGAGTTCACTGGCGCTTTG$^{4254(M14758)}$	(−) RT-PCR/F.4B1
GAPDH-F§	5′-CGGCTACTAGCGGTTTTACG-3′	ChIP/F. 5D1,D2
GAPDH-R§	5′-AAGAAGATGCGGCTGACTGT-3′	ChIP/F. 5D1,D2

Abbreviations: ECW and ECP, the regions designated for the *ABCB1* upstream primers as indicated in Fig. 5*A*; Exp., experiments listed in this study; F, forward primer; GSP, gene-specific primer; P1, the *ABCB1* proximal promoter; ChIP, chromatin immunoprecipitation.

*The cDNA sequences from the genes upstream of *ABCB1* were based on the sequences with indicated accession numbers. The positive/minus (+/−) strands are indicated in the amplimers' sequences.

† DNA amplimers were designated according to the *H. sapiens* BAC clone CTB-60P12 from chromosome 7 (accession no. AC002457). The underlined sequences represent restriction sites to facilitate PCR subcloning.

‡ *ABCB1* coding region primers were based on the sequences from the accession no. M14758.

§ *GAPDH* promoter region primers were obtained from Upstate Cell Signaling Solution.

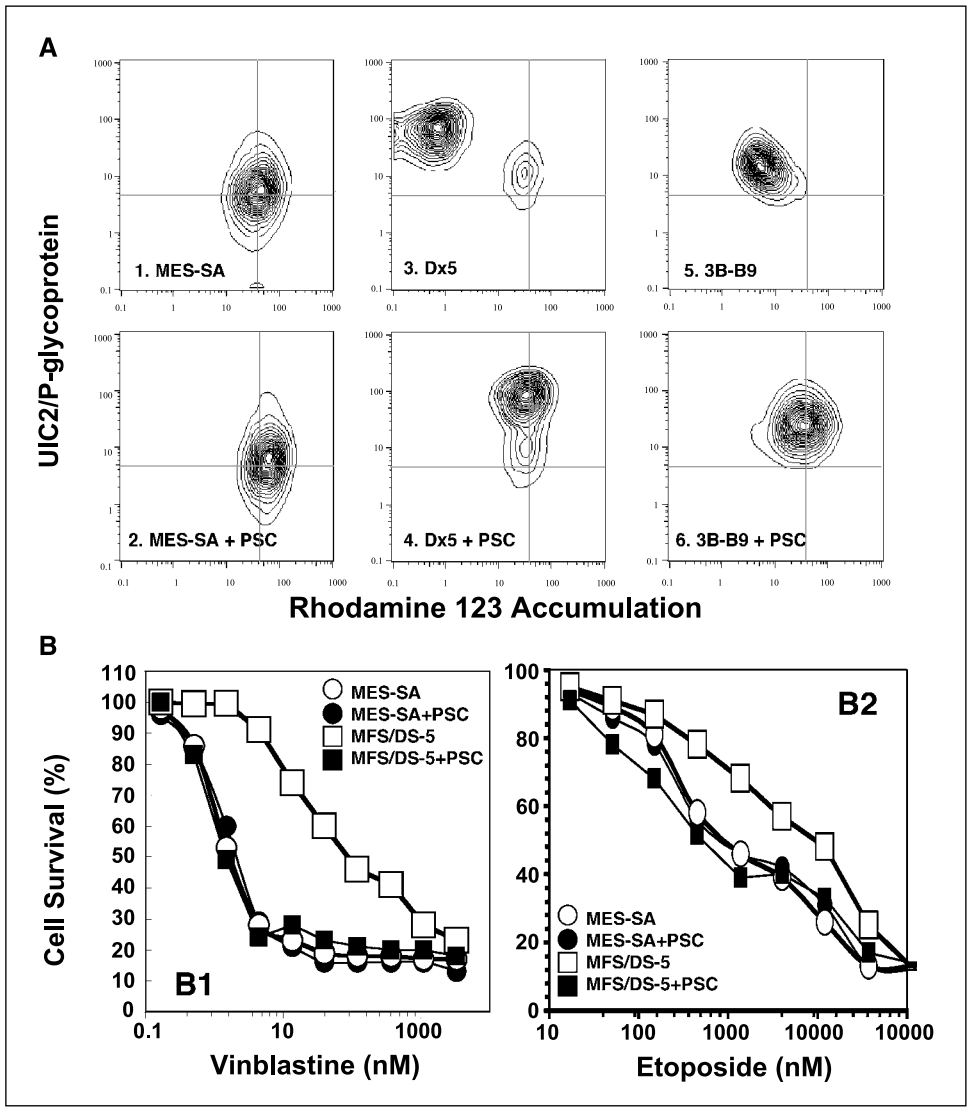

Figure 1. Functional analysis of the MDR phenotype. *A,* flow cytometry. Double labeling of MES-SA (negative control), Dx5 (positive control), and one representative DSM (e.g., 3B-B9) with both Rh-123 and the monoclonal antibody UIC2 in the presence (A2, A4, and A6) or absence (A1, A3, and A5) of 2 μmol/L PSC was done as described and analyzed by the FlowJo software (Stanford University). *B,* 3-(4,5-dimethylthiazol-2-yl)-2,5-diphenyltetrazolium bromide assay of drug sensitivity (Table 1) of the DSM mutants. One representative clone (MFS/DS5) obtained by 80 nmol/L doxorubicin selection for 2 weeks is shown.

prevalent *ABCB1* activation in MES-SA cells (6). We selected those DSMs that had stable *ABCB1* expression to test their resistance to the selecting agent doxorubicin as well as to vinblastine and VP-16. In general, the MDR phenotype in DSMs was similar to that which we previously reported (6). Functional expression of P-glycoprotein in the DSM was confirmed by flow cytometry using the UIC2 monoclonal antibody and Rh-123 (Fig. 1*A, right*). The multiply selected, highly MDR variant Dx5 cells were used as *ABCB1*-positive controls in these studies. The partial reversion exhibited by Dx5 cells in this figure is evidence of multiple genetic steps in the evolution of those cells (Fig. 1*A, middle*). We also derived new DSM clones (e.g., MFS/DS-5) from an MES-SA subclone (MFS). These subclones displayed a typical MDR phenotype that can be completely reversed to the level of parental MES-SA cells by the P-glycoprotein inhibitor PSC833 (PSC), suggesting that activation of the *ABCB1* gene is the predominant resistant mechanism in these drug-resistant MES-SA cells (Fig. 1*B*). We also isolated the doxorubicin-induced variants via a 6-day doxorubicin sublethal induction. A detailed description of both doxorubicin-selected and doxorubicin-induced variants is provided in Table 1 and in Supplementary Fig. 1.

Molecular characterization of *ABCB1* activation in doxorubicin single-step-selected mutants. Molecular characterization of the DSMs was done and is depicted in Fig. 2. As shown in Fig. 2*A*, the *ABCB1* gene was amplified 4-fold in the multistep-selected Dx5 cell line (*lane 5*), relative to its parental drug-sensitive MES-SA cells as determined by Southern blot. There is also a rearranged fragment on or around the *ABCB1* promoter in Dx5 cells. However, neither *ABCB1* gene amplification nor gene rearrangement was observed in the DSMs (*lanes 2-4*). In addition, we found no changes in gene copy numbers in genes upstream of *ABCB1* (e.g., *RPIB9* and *MCFP*) by real-time PCR (data not shown). These data suggest that either genomic alterations outside the *ABCB1* promoter or transcriptional activation of *ABCB1* might be important in these DSMs (see Supplementary notes for Fig. 2*A*).

We further mapped the transcription start site(s) and showed that the native *ABCB1* P1 promoter protects 130- and 134-bp fragments in Dx5 cells (Fig. 2*C, lane 5*), but, surprisingly, not in those single-step mutants (2B-E3, 3B-B9, and 10B-E2) in which a ~324-bp mRNA fragment was protected (Fig. 2*C, lanes 2-4*), indicating that the *ABCB1* gene is predominantly initiated from upstream sites in these single-step mutants. To confirm

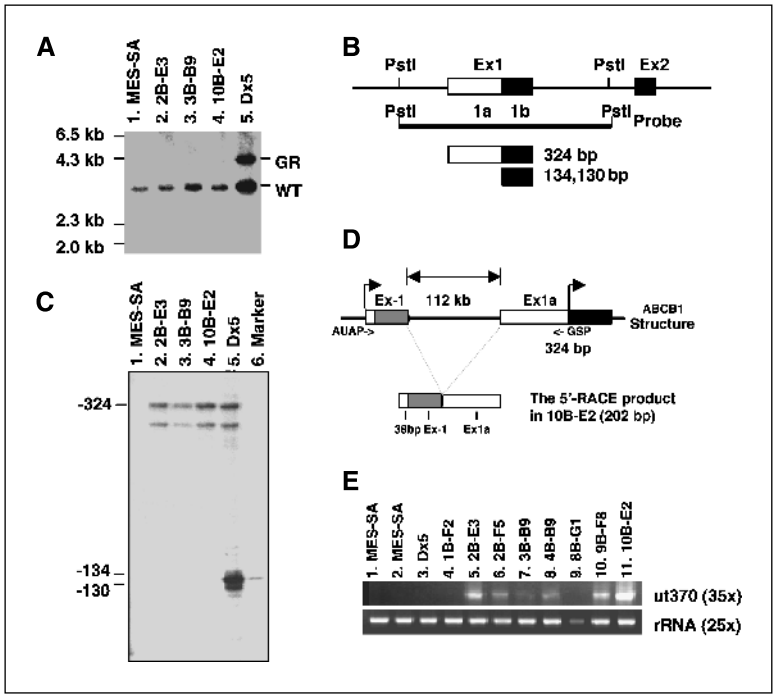

Figure 2. Molecular characterization of the DSMs. *A,* Southern blot. Fifty micrograms of genomic DNAs from MES-SA, its DSMs, and Dx5 cells were digested by *Hin*dIII, 1% agarose gel-fractionated, transferred onto a nylon membrane, and hybridized with the *Pst*I-*Pst*I fragment of the *ABCB1* promoter labeled by [α-^{32}P]-dCTP as referenced in Materials and Methods. Abbreviations: GR, the *ABCB1* gene rearrangement; WT, the wild-type *ABCB1* genomic structure. *B,* structure of the *Pst*I-*Pst*I probe (982 bp) of the *ABCB1* P1 promoter used in RNase protection assays and the protected mRNA fragments from exon 1 (Ex1). *C,* RNase protection assay. The assay was done with parental MES-SA cells (negative controls), Dx5 (positive control), and the three DSMs (2B-E3, 3B-B9, and 10B-E2). Total RNAs were hybridized with the antisense RNA probe. Transcripts starting at the native *ABCB1* P1 protect a 130- or 134-bp fragment. mRNAs with start sites 5′ to these protect a 324-bp fragment as indicated. *D,* confirmation of far upstream sequences by 5′-RACE in the DSM. The 202-bp 5′-RACE fragment (RACE202) from the DSM (10B-E2) was isolated by 5′-RACE protocols, which is composed of 70 bp of exon 1a, 94 bp of exon −1, and an additional 38 bp upstream of exon −1 of the *ABCB1* gene. Abbreviations: AUAP, abridged universal anchor primer; GSP, gene-specific primer. *E,* RT-PCR analysis of ut370 in DSMs. MES-SA cells (*lanes 1-2*) were negative controls. *Lanes 4-11,* DSMs. PCR cycle numbers (*x*) are indicated.

the initiation site(s) of upstream *ABCB1* transcripts in the DSMs (accession no. AF345625), we did 5′-RACE and isolated a 202-bp fragment (designated as RACE202) from a DSM, 10B-E2. Sequencing revealed that this band was homologous to two regions of the *Homo sapiens* BAC clone CTB-060P12 from 7q21. The mRNAs in the DSMs represent far upstream transcripts containing the previously described exon −1 of *ABCB1* (17, 18), which is transcribed from a locus that is 112 kb away from the *ABCB1* P1 promoter (Fig. 2*D*). To verify the prevalence of the upstream transcripts in MDR cellular models, we designed specific primers to detect the transcripts containing exon −1. These primers generate a 370-bp RT-PCR product (ut370), which includes exon −1 (94 bp) and exon 1 (276 bp) as shown in Fig. 2*D* and in Supplementary Fig. 2. Transcripts originating at the upstream site were evident in 71% (five of seven) of DSMs but not in Dx5 cells (Fig. 2*E*; Supplementary notes for Fig. 2*E*).

Identification of the spontaneous nature of ut370 in MES-SA cells. We have previously shown that either doxorubicin or vinblastine selects spontaneous *ABCB1* mutants in MES-SA cells (6, 9). To test whether activation of the *ABCB1* upstream transcripts occur spontaneously in MES-SA sarcoma cells, we examined the presence or absence of the upstream transcripts in bulk MES-SA cells. Our data revealed that the *ABCB1* upstream transcripts were detectable only after 40 cycles of PCR amplification in some batches (5×10^6 cells per batch, obtained from different passages) of MES-SA cells with a frequency of two of nine (Fig. 3*B, lanes 4-8*, four of nine batches of MES-SA cells are shown). To show the spontaneous nature of this upstream transcript (ut370), we isolated a panel of MES-SA subclones by limiting dilution. One clone, termed MES-SA/FS (MFS), displayed a karyotype similar to its parental MES-SA cells (14), and expressed the *ABCB1* upstream transcripts (ut370) detectable by 40 cycles of PCR amplification (Fig. 3*B, lane 4*). Moreover, the ratio of the *ABCB1* upstream transcripts between MFS cells and a vinblastine-resistant clone (Fig. 3*B, lane 3*, a positive control) was ~1 to 32, implying that only a small portion of MFS cells acquired transcripts from upstream promoter during clonal expansion (Fig. 3*A, open oval*). Neither *ABCB1* mRNA expression (determined by 50 cycles of RT-PCR; Fig. 3*C*) nor P-glycoprotein expression (data not shown) was observed in MFS cells, suggesting that the acquisition of the upstream transcript (ut370) does not warrant a fully activated *ABCB1* in these cells.

Complete activation of *ABCB1* requires drug selection of the upstream *ABCB1*. To determine whether *ABCB1* activation occurs preferentially in the preexisting spontaneous mutants (with ut370), we exposed MFS cells to the MDR substrates vinblastine and doxorubicin (Fig. 3*A*). The drug-resistant phenotype for vinblastine selection has been fully characterized (9). In general, both MFS/vinblastine single-step mutants (VSM) and MFS/DSMs displayed a typical MDR phenotype related to *ABCB1* activation (Fig. 1; Table 1; ref. 9). As we expected, the MDR phenotype in these cells was associated with expression of ut370 in both the MFS/VSM (eight of eight, Fig. 3*D*) and MFS/DSM variants (four of four, with only three clones presented in Fig. 3*E*). Of note, VP-16, a weaker substrate for P-glycoprotein, failed to induce transcription from the upstream promoter and thus resulted in the selection of non-*ABCB1*-resistant mechanisms (Fig. 3*E, lane 7*). The ut370 mRNAs were also confirmed by sequencing analysis (accession nos. AF345624 and AF345623). Neither short-term (Supplementary Fig. 3) nor sublethal doxorubicin induction (Fig. 3*F*) induces *ABCB1* transcripts originated at the upstream promoter in MES-SA cells. Taken together, these data suggest *ABCB1* activation in DSMs occurs as a result of the initiation of transcription at the *ABCB1* far upstream promoter, and that additional mechanisms are induced during the course of single-step selection that promote *ABCB1* transcription through the native, proximal *ABCB1* promoter.

Activated *RPIB9* mRNA expression correlated with *ABCB1* expression. To verify whether the initiation of upstream transcripts was associated with transcriptional activity of the genes upstream of the *ABCB1*, we did real-time RT-PCR analysis of mRNA expression for both *MCFP* (*H. sapiens* mitochondrial carrier family protein, accession no. AF125531) and *RPIB9* (*H. sapiens* Rap2-binding protein 9, accession no. BC022520), which are located

upstream of exon −1 of *ABCB1* (Fig. 4*A*). The *MCFP* gene is transcribed from a region that is ~123 kb upstream of the upstream transcripts, whereas the *RPIB9* gene is transcribed from the DNA strand opposite to the upstream transcripts and *ABCB1*. As shown in Fig. 4*B*, *MCFP* mRNA levels were increased (by 1.3- to 2.4-fold) in several drug-selected cell lines except 3B-B9. The expression pattern of *MCFP* was correlated with *ABCB1* expression in the DSMs (10B-E2, 2B-E3, 3B-B9, and MFS/DS5) but not in multistep-selected Dx5 cells (Fig. 4*B1* and *B2*). Furthermore, the expression pattern of *RPIB9* was tightly correlated with *ABCB1* expression, in that the mRNA ratios of *RPIB9* expression in the four DSMs (10B-E2, 2B-E3, 3B-B9, and MFS/DS5) are 1:4.6:1.3:3, values that were consistent with those of *ABCB1* (1:4.7:2.0:3.4; Fig. 4*B*). However, Dx5 cells did not express *RPIB9*, also consistent with the observation that Dx5 cells lack the upstream transcript (ut370). These data suggest that regional gene transcriptional activity may be associated with *ABCB1* expression by altering regional chromatin structures that affect *ABCB1* upstream transcription.

Chromatin remodeling by acetylated H3. To determine whether remodeling of chromatin structures by posttranslational modification of the structure of nucleosomes plays a role in activating the *ABCB1* far upstream promoter region, we examined the acetylation status of the core histone protein H3 by chromatin immunoprecipitation assays using an anti-acetylated H3 antibody in MES-SA, two DSMs (2B-E3 and 10B-E2), and Dx5 cells. Acetylation of H3 histones within the 968 bp upstream of exon −1 was markedly increased by 18- and 25-fold, respectively, in 10B-E2 and 2B-E3, but only 1.7-fold in Dx5 cells compared with parental MES-SA cells (Fig. 5*D3*) as determined by at least five sets of primers that cover this area (described in Table 2 and partially listed in Fig. 5*A*). Modification of histone H3 was not evident in the 622-bp region upstream of the acetylated 968-bp region (Fig. 5*D4*). A reciprocal pattern of acetylation of histone H3 was observed in the *ABCB1* P1 promoter region, in which Dx5 displayed a 35-fold increase in acetylated H3 as determined by real-time PCR using the five primer sets that cover the *ABCB1* promoter region (Table 2,

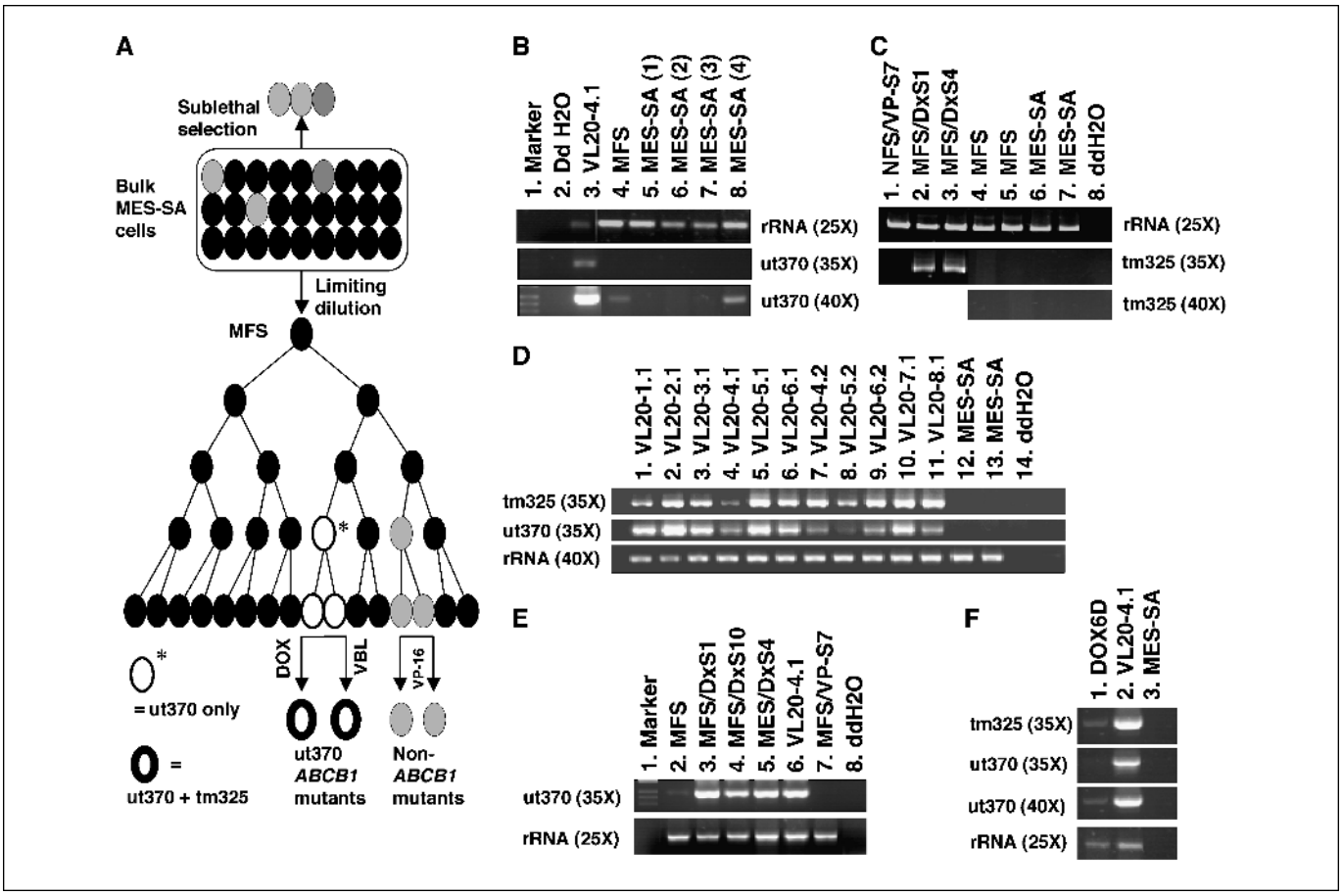

Figure 3. Selection of spontaneous mutants with the *ABCB1* upstream transcripts. *A,* schematic presentation of the isolation of the MES-SA subclone and single-step selection or sublethal selection by multiple anticancer drugs. The subclonal cell line MFS, generated from MES-SA cells by the limiting dilution method, was used for fluctuation analysis and single-step-selection by vinblastine (9), doxorubicin (in this study), and VP-16 (in this study). *Open oval,* spontaneous mutant cells with ut370 arisen from MFS cells. *Open oval with bolded outlines,* clones with both the *ABCB1* upstream and downstream transcripts. Abbreviations: DOX, doxorubicin; VBL, vinblastine; VP, VP-16. *B,* RT-PCR analysis of ut370 in bulk MES-SA cells and in the MES-SA subclone (MFS). Different batches of MES-SA cells (four of nine, *lanes 5-8*) were included. *C,* analysis of expression of *ABCB1* mRNA at coding regions was done by using primers spanning transmembrane 6 of the *ABCB1* gene (9). The designated products were tm325. *D,* analysis of both tm325 (*top*) and ut370 (*middle*) in VSMs derived from MFS cells (*lanes 1-11*). Parental MES-SA cells (*lanes 12-13*) were used as negative controls. *E,* RT-PCR analysis of ut370 was done in the DSMs derived from MFS cells (*lanes 3-5*). MFS/VL20-4.1 (obtained by selection with 20 nmol/L vinblastine) and MFS/VP-S7 (obtained by selection with 0.5 μmol/L VP-16) were used as an *ABCB1*-positive and *ABCB1*-negative control, respectively, in this experiment. *F,* RT-PCR analysis of both ut370 and tm325 expression was carried out in the variant (MES-SA/DOX6D or DOX6D) derived from doxorubicin (80 nmol/L) sublethal exposure for 6 days. MES-SA and MFS/VL20-4.1 cells were used as a negative and positive control for both tm325 and ut370, respectively. rRNA was used as the control gene to normalize sample loading. The samples were analyzed by a 2% agarose gel and stained with ethidium bromide.

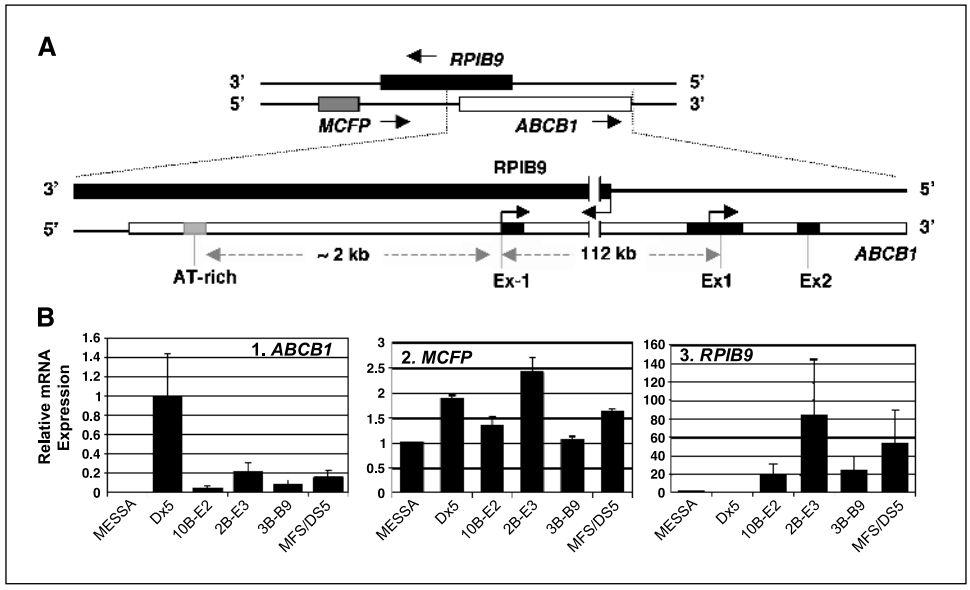

Figure 4. Real-time PCR analysis of mRNA expression of the genes (*MCFP* and *RPIB9*) upstream of *ABCB1*. *A,* a physical map of *ABCB1* and its upstream genes. *RPIB9* is located on the opposite DNA strand of *ABCB1*, in which *RPIB9* partially overlaps with the far upstream region of *ABCB1*. The *MCFP* gene is localized at a region that is ~123 kb upstream of exon −1 of the *ABCB1* gene. *B,* relative *ABCB1, MFCP*, and *RPIB9* mRNA expression in MES-SA and its MDR derivatives. The mRNA expression was normalized to *GAPDH* expression. *Columns* (*B1-B3*), means of relative RT-PCR products from three independent amplifications; *bars,* SD. One of two independent experiments done in triplicate is shown.

Fig. 5*D*). Thus, these data confirmed that *ABCB1* activation in DSMs and Dx5 cells occurs at distinct sites in the 7q21 chromosomal region, although they may share some similar mechanisms such as acetylation of histone H3. However, initiation of *ABCB1* transcription at the downstream promoter is controlled by an initiator sequence and transcriptional factors on the *ABCB1* promoter (12), whereas the 320-bp region upstream of the exon −1 lacks typical promoter elements such as a TATA box and also lacks initiator sequences and DNA binding consensus for transcriptional factors (analysis not shown). Thus, how transcription initiation is mediated by RNA polymerase II in the *ABCB1* upstream region remains obscure.

Functional analysis of the *ABCB1* far upstream region and the *ABCB1* P1 promoter. To determine whether the *ABCB1* upstream transcripts represented a simple activation of an upstream promoter (P2), we used the putative promoter (P2)-CAT construct (ECP2-370) containing the 370-bp sequences upstream of exon −1 of *ABCB1* to examine promoter activity in both MES-SA and its MDR variants (e.g., 10B-E2) that express the upstream transcripts (ut370). CAT activity was also compared with both the SV40 promoter and the *ABCB1* P1 promoter (DC-1018). As shown in Fig. 6*A*, the electroporation experiment did not reveal significant basal promoter activity (~1.3-fold related to the vector control) with the ECP2-370 construct (Fig. 6*A*, *columns 1-2*) in MES-SA cells compared with both the SV40 and the *ABCB1* promoter which displayed 6.3- and 8.4-fold CAT activity when compared with the vector control (Fig. 6*A, columns 1, 3*, and *4*). There was only a 1.5-fold increase in CAT activity in the ECP2-370 vector transiently transfected into the DSM 10B-E2 (Fig. 6*B, columns 2* and *4*). Moreover, we also observed similar results in 2B-E3 and two MFS/VSM variants (MFS/VL20-3.1 and MFS/VL20-6.1; data not shown). These data indicate that the upstream region in MES-SA cells lacks basal promoter activity in contrast with the *ABCB1* P1 promoter that has a strong basal transcriptional activity in MES-SA cells.

We further examined *ABCB1* P1 promoter activity in 10B-E2 cells maintained in drug-free medium and only found a 1.5-fold increase in *ABCB1* P1 promoter activity in 10B-E2 cells compared with MES-SA control (data not shown). Furthermore, we evaluated the *ABCB1* basal promoter in parental MES-SA cells (Fig. 6*C, lanes 1-2*) and in drug-selected/induced sublines (Fig. 6*C, lanes 3-10*) by transiently introducing the *ABCB1* reporter plasmid into these cells. Basal and drug-selected/induced *ABCB1* promoter activity in the plasmid reflects the reactivity of transcriptional factors that act on the *ABCB1* reporter construct and thus mimics the open chromatin of the *ABCB1* promoter but not that of the chromatin-embedded *ABCB1* promoter. This basal promoter activity could be significantly modulated under drug selection conditions in sister clones (e.g., 10B-C5) as determined by quantitative analysis [^{14}C]-labeled acetyl chloramphenicol species (Fig. 6*C-D*). This revealed 5- to 12-fold increases in *ABCB1* P1 promoter activity in the DSMs, comparable with that in Dx5 (Fig. 6*D*), suggesting an interaction of either transcriptional factors or other epigenetic mechanisms with the *ABCB1* P1 promoter during drug selection.

Discussion

The model for the activation of *ABCB1* in MES-SA cells, based on our experimental data, is illustrated in Fig. 7. In this model, the single-step selection favors the isolation of clones with a spontaneous alteration that generates *ABCB1* upstream transcripts (a partially activated *ABCB1* status). It seems that an initial event contributes to an altered epigenetic mechanism (i.e., a major increase in acetylated H3 that modifies the chromatin structure of the *ABCB1* far upstream region and thus initiates *ABCB1* upstream transcripts). In MES-SA cells, MDR clones arise as a result of altered chromatin remodeling in the region of the upstream promoter.

Acquisition of spontaneous mutants as a discrete genetic step for ABCB1 activation. We previously hypothesized that a major genomic instability (with a mutation rate of 1.8×10^{-6} per cell per generation) leads to *ABCB1* activation in DSM cells, based on fluctuation analyses (6). In this study, we were able to provide direct evidence supporting this hypothesis (Fig. 3). *ABCB1* upstream transcripts are evident after 40 cycles of RT-PCR amplification in some bulk MES-SA cells and in the MFS clonal variant of the MES-SA cell line (Fig. 3*B*). MFS cells were derived by expanding one single cell to several million cells without any drug

selection thus providing experimental evidence that the upstream *ABCB1* transcripts are spontaneous in nature, as defined by a spontaneous mutation rate (6, 9). However, the exact change that is responsible for the generation of the *ABCB1* upstream transcript is unknown. It might be associated with genomic instability of *ABCB1* upstream DNA sequences, which in turn affects the local chromatin structure around exon −1 or chromosomal alterations outside chromosome 7. These changes could result in expression of altered transcription factors that regulate the chromatin-remodeling processes or modify the histone core of nucleosomes in the region around the *ABCB1* upstream promoter (Fig. 7*B*).

A mutational event contributes to epigenetic modification of the histone core. We have shown that acetylated H3 was dramatically increased in the single-step mutants in a 968-bp region upstream of the promoter region, where *ABCB1* upstream transcripts are generated. In eukaryotes, the basic unit of chromatin structures is assembled by wrapping ~150 bp of DNA around histone octamers that are composed of four histone heterodimers (two each of H3-H4 and H2A-H2B). It has been well established in many cellular models that both deacetylation and acetylation of histones play a central role in gene regulation (12, 19–21). Our data suggest that an increase in acetylated H3 in the nucleosomes within the 968-bp upstream region proximal to the *ABCB1* upstream promoter is one important step to open the chromatin structure, which in turn provides the accessibility for basal transcriptional machinery to act on exposed DNA and thus initiates gene transcription. The initiation of upstream transcripts may also depend on the acetylated region that interacts with local chromosomal/chromatin structures and distal enhancer elements. Whether a gain-of-function mutation of histone acetyltransferases, a loss-of-function mutation of histone deacetylases, or another alteration is the initial driving force to initiate transcription from the upstream promoter is unknown.

Upstream transcriptional activity correlates with *ABCB1* mRNA expression. It has been shown that *ABCB1* activation can be achieved by capturing a hybrid *ABCB1* mRNA. In these cases, the hybrid partner usually originated from a region far upstream of exon −1 of the *ABCB1* gene in chromosome 7 or from another chromosome following a rearrangement (15, 22). We found an association of both *MCFP* and *RPIB9* expression with *ABCB1* expression in our MDR cellular models (Fig. 4*B*). The functions of both *MCFP* and *RPIB9* are largely unknown (23). The tight correlation of *RPIB9* and *ABCB1* gene expression pattern in the DSMs, but not the multistep-selected Dx5 cells that lack the ut370 upstream transcripts (Fig. 4*C*), suggests that transcription of *ABCB1* from the upstream promoter and transcription of the *RPIB9*

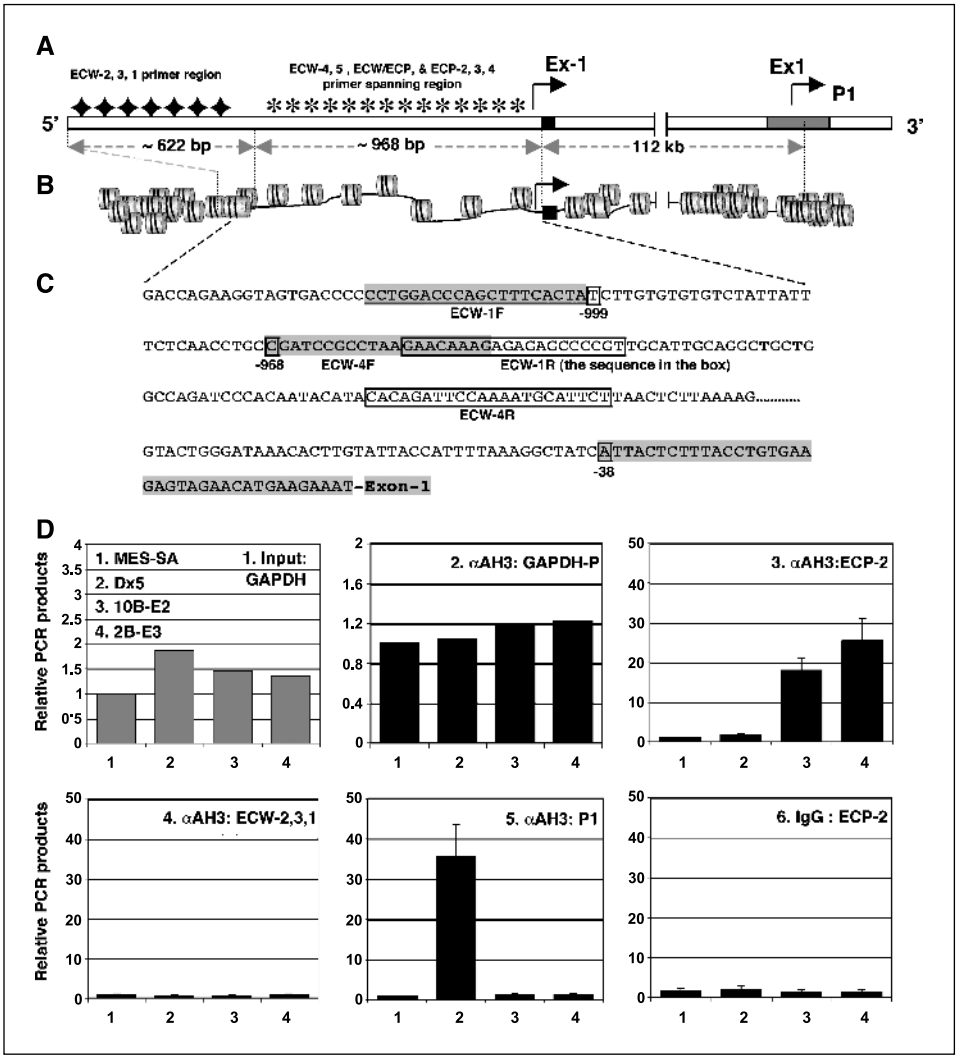

Figure 5. Chromatin immunoprecipitation assays of chromatin status with the anti-acetylated H3 antibody. *A,* a physical map of both the *ABCB1* upstream and downstream regions. The primer locations were labeled, with increased acetylated H3 in nucleosomes relative to MES-SA control (✻) and unacetylated H3 (♦) indicated. *B,* schema of the deduced chromatin structure around exon −1 of the *ABCB1* gene. *C,* genomic DNA sequences of the 968-bp region upstream of exon −1 with partial primer sequences indicated for real-time PCR. *D,* chromatin immunoprecipitation and real-time PCR analysis of the precipitated genomic DNA sequences. *D1,* input control. Sonicated genomic DNAs without the chromatin immunoprecipitation steps and amplified with the glyceraldehyde-3-phosphate dehydrogenase (*GAPDH*) promoter primer as listed in Table 2. *D2-D5,* chromatin immunoprecipitation assays with the anti-acetylated H3 antibody (αAH3) and real-time PCR analysis using ECP2, ECW, and *ABCB1* P1 promoter primers (Table 2), respectively. *D6,* chromatin immunoprecipitation assays with rabbit IgG (control) and real-time PCR analysis using the ECP-2 primer. The result was normalized to the *GADPH* promoter control in each reaction. One of three independent experiments with triplicate is shown.

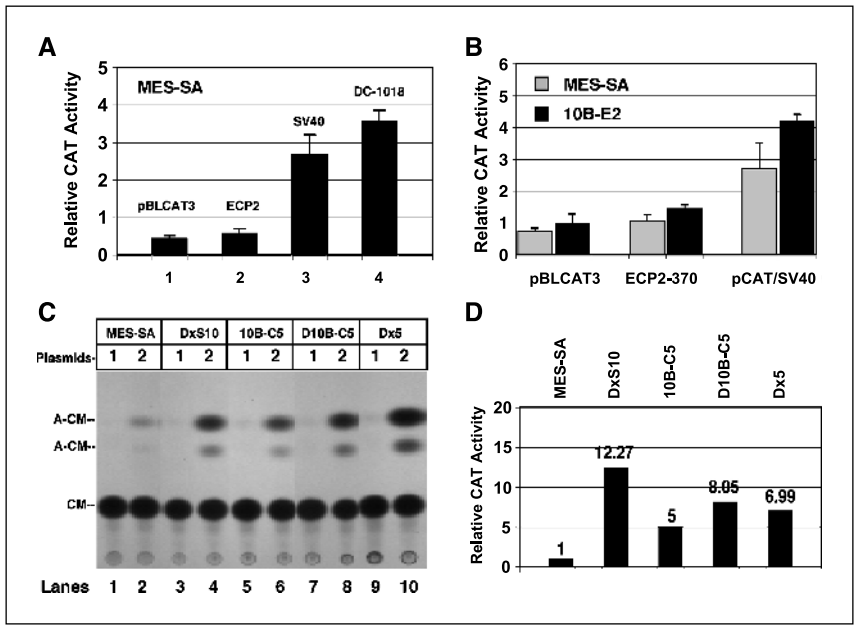

Figure 6. Analysis of CAT activity of the upstream region of exon −1 and the *ABCB1* P1 promoter in MES-SA and its drug-resistant derivatives. *A,* CAT ELISA assays of basal promoter activity of the upstream region (around exon −1, ECP2-370 or ECP2), the *ABCB1* P1 promoter (DC-1018), and the SV40 promoter (pCAT/SV40, SV40). *B,* CAT ELISA assays of drug-selected or drug-induced promoter activity of the upstream region (around exon −1), the *ABCB1* P1 promoter, and the SV40 promoter in the DSM 10B-E2. *C,* analysis of *ABCB1* P1 promoter activity by transient transfection of pBLCAT3 (control = 1) and the *ABCB1*-CAT vector (DC-1018 = 2) into the DSMs (DxS10 and 10B-C5), 0.5 μmol/L doxorubicin-induced 10B-C5 cells (D10B-C5), and Dx5. MES-SA cells were used as control in this experiment. The pSV-β-galactosidase plasmid was used an internal control for electroporation efficiency in these CAT assays. *D,* relative CAT activity of (*C*) was determined by the [^{14}C] scintillation counts of acetylated chloramphenicols (*A-CM*) and normalized to β-galactosidase expression levels. At least one of three independent experiments is shown.

gene on the same chromosome 7 are initiated concurrently. The increased transcriptional activities at 7q21 might be result from alterations of regional chromatin structures within the 112-kb intronic sequences, upstream of the *ABCB1* gene, that promote transcription through barriers in this region. It might also provide enhancer elements to facilitate *ABCB1* transcription from the upstream promoter. Further study is needed to verify these possibilities.

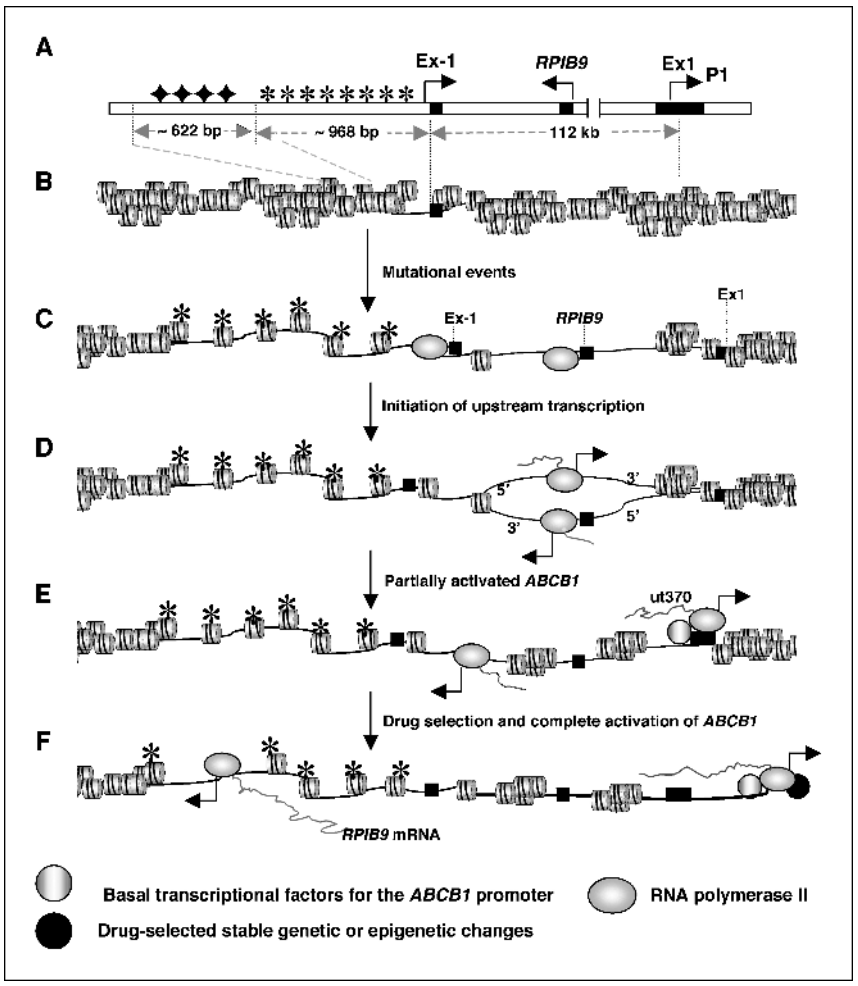

Figure 7. Schematic model of the origins of MDR cells in cancer. The genetic and epigenetic steps (*B-F*) that are required to develop MDR cells in a MES-SA sarcoma are diagrammed. *A, ABCB1* genomic organization at 7q21 with *ABCB1* far upstream (around exon −1) and the *ABCB1* promoter (Ex1a and Ex1b), *B,* a nucleosomal representation of the *ABCB1* genomic organization corresponding to (*A*) with both the genomic instability region around exon −1 and the chromatin-embedded *ABCB1* promoter indicated. *C,* spontaneous mutations promote the acetylation of histone H3. *D,* the initiation of the upstream transcript containing exon −1 associated with regional transcriptional activity (e.g., *RPIB9* activation). *E,* partially activated *ABCB1* status with the transcript (containing ut370) terminated on the *ABCB1* promoter, which is likely suppressed by the packed chromatin of the *ABCB1* promoter. *F,* complete activation of *ABCB1* may be achieved by either altered transcriptional factors (such as Sp1, AP1, NF-Y, YB-1, and C/EBPβ; refs. 12, 16) that interact with the *ABCB1* promoter or epigenetic changes of the *ABCB1* chromatin. These transcriptional and epigenetic changes, which may be acquired during the course of drug selection, permit transcriptional activation of the endogenous and chromatin-embedded *ABCB1* promoter.

Interplay between genetic and epigenetic mechanisms at the *ABCB1* promoter. Unselected MES-SA cells that contain transcripts originating at the upstream *ABCB1* promoter lack *ABCB1* mRNAs encompassing the coding regions, suggesting that the *ABCB1* gene is not fully activated without drug selection (Fig. 3*B-C* and Fig. 7*E*). Thus, it seems that in some cases, the selection of preexisting mutations or epigenetic changes by chemotherapeutic agents (such as vinblastine, doxorubicin, or paclitaxel) is needed to give rise to a fully activated *ABCB1* in these spontaneous mutants (Fig. 3*D-E* and Fig. 7*F*). Indeed, *ABCB1* promoter activity was increased in the DSMs that are maintained in drug selection conditions, and this was significantly modulated in the presence of higher doxorubicin concentrations (e.g., 0.5 μmol/L doxorubicin; Fig. 6*C-D*). This suggests that additional *trans*-alterations (mediated by doxorubicin) act on the open chromatin structure of the *ABCB1* promoter in the DSM cells to facilitate transcription from the *ABCB1* promoter thus achieving complete activation of *ABCB1*. *Trans*-alterations that are involved in the above processes might include stable or transient expression or down-regulation of a panel of transcriptional factors. The stability of the MDR phenotype of the DSMs cultured in drug-free medium rules out transient expression (induction) of transcriptional factors as a major mechanism for *ABCB1* expression in these cells (Table 1). The nature of the heritable changes that result in these stable MDR variants is not known but may include stable expression of transcription factors interacting with the *ABCB1* promoter, drug-induced acetylation of other histones, and demethylation of the *ABCB1* promoter.

In summary, our data suggest that *ABCB1* expression in these single-step mutants arose from a discrete genetic step contributing to epigenetic modification of the histone core H3-initiating transcription from the *ABCB1* upstream promoter. Transcriptional activity of the genes upstream of *ABCB1* may be associated with *ABCB1* mRNA expression. We conclude that interplay between genetic and epigenetic mechanisms at the putative *ABCB1* upstream promoter and in the region proximal to this contributes to complete activation of *ABCB1* in some cancer cells.

Acknowledgments

Received 11/17/2004; revised 8/3/2005; accepted 8/8/2005.

Grant support: NIH grant R01-CA92474 (B.I. Sikic) and National Cancer Institute grant CA09302 (K.G. Chen and M.E. Schaner).

The costs of publication of this article were defrayed in part by the payment of page charges. This article must therefore be hereby marked *advertisement* in accordance with 18 U.S.C. Section 1734 solely to indicate this fact.

References

1. Luria SE, Delbrück M. Mutations of bacteria from virus sensitive to virus resistance. Genetics 1943;28:491–511.
2. Goldie JH, Coldman AJ. A mathematic model for relating the drug sensitivity of tumors to their spontaneous mutation rate. Cancer Treat Rep 1979;63: 1727–33.
3. Kendal WS, Frost P. Pitfalls and practice of Luria-Delbrück fluctuation analysis: a review. Cancer Res 1988; 48:1060–5.
4. Lenski RE, Mittler JE. The directed mutation controversy and neo-Darwinism. Science 1993;259:188–94.
5. Biedler JL, Spengler BA. Genetics of drug resistance. In: Goldstein LJ, Ozols RF, editors. Anticancer drug resistance: advances in molecular and clinical research. Norwell (Massachusetts): Kluwer Academic Publishers; 1994. p. 1–16.
6. Chen G, Jaffrezou JP, Fleming WH, Duran GE, Sikic BI. Prevalence of multidrug resistance related to activation of the *mdr1* gene in human sarcoma mutants derived by single-step doxorubicin selection. Cancer Res 1994;54: 4980–7.
7. Beketic-Oreskovic L, Duran GE, Chen G, Dumontet C, Sikic BI. Decreased mutation rate for cellular resistance to doxorubicin and suppression of *mdr1* gene activation by the cyclosporin PSC 833. J Natl Cancer Inst 1995;87: 1593–602.
8. Dumontet C, Duran GE, Steger KA, Beketic-Oreskovic L, Sikic BI. Resistance mechanisms in human sarcoma mutants derived by single-step exposure to paclitaxel (Taxol). Cancer Res 1996;56:1091–7.
9. Chen GK, Duran GE, Mangili A, Beketic-Oreskovic L, Sikic BI. *MDR*1 activation is the predominant resistance mechanism selected by vinblastine in MES-SA cells. Br J Cancer 2000;83:892–8.
10. Ling V. P-glycoprotein and resistance to anticancer drugs. Cancer 1992;69:2603–9.
11. Gottesman MM, Fojo T, Bates SE. Multidrug resistance in cancer: role of ATP-dependent transporters. Nat Rev Cancer 2002;2:48–58.
12. Scotto KW. Transcriptional regulation of ABC drug transporters. Oncogene 2003;22:7496–511.
13. Chen G, Duran GE, Steger KA, et al. Multidrug-resistant human sarcoma cells with a mutant P-glycoprotein, altered phenotype, and resistance to cyclosporins. J Biol Chem 1997;272:5974–82.
14. Chen GK, Lacayo NJ, Duran GE, et al. Preferential expression of a mutant allele of the amplified *MDR*1 (*ABCB1*) gene in drug-resistant variants of a human sarcoma. Genes Chromosomes Cancer 2002;34:372–83.
15. Mickley LA, Spengler BA, Knutsen TA, Biedler JL, Fojo T. Gene rearrangement: a novel mechanism for *MDR-1* gene activation. J Clin Invest 1997;99: 1947–57.
16. Chen GK, Sale S, Tan T, Ermoian RP, Sikic BI. CCAAT/enhancer-binding protein β (nuclear factor for interleukin 6) transactivates the human *MDR1* gene by interaction with an inverted CCAAT box in human cancer cells. Mol Pharmacol 2004;65:906–16.
17. Chen CJ, Chin JE, Ueda K, et al. Internal duplication and homology with bacterial transport proteins in the *mdr1* (*P-glycoprotein*) gene from multidrug-resistant human cells. Cell 1986;47:381–9.
18. Ueda K, Clark DP, Chen CJ, et al. The human multidrug resistance (*mdr1*) gene. cDNA cloning and transcription initiation. J Biol Chem 1987;262: 505–8.
19. Struhl K. Histone acetylation and transcriptional regulatory mechanisms. Genes Dev 1998;12:599–606.
20. Ruijter AJ, van Gennip AH, Caron HN, Kemp S, van Kuilenburg AB. Histone deacetylases (HDACs): characterization of the classical HDAC family. Biochem J 2003; 370:737–49.
21. Jin S, Scotto KW. Transcriptional regulation of the *MDR1* gene by histone acetyltransferase and deacetylase is mediated by NF-Y. Mol Cell Biol 1998;18:4377–84.
22. Mickley LA, Lee JS, Weng Z, et al, Genetic polymorphism in *MDR-1*: a tool for examining allelic expression in normal cells, unselected and drug-selected cell lines, and human tumors. Blood 1998;91:1749–56.
23. Wang S, Zhang Z, Ying K, et al. Cloning, expression, and genomic structure of a novel human Rap2 interacting gene (*RPIP9*). Biochem Genet 2003;41:13–25.